ADSORPTION MODELING ON CARBON MONOLITHIC COLUMN
FOR METHYLENE BLUE REMOVAL

PEMODELAN PENYERAPAN PADA KOLOM MONOLITIK BERLAPIS KARBON
UNTUK PEMISAHAN METILEN BIRU

Darmadi*, Medyan Riza, and Mirna Rahmah Lubis

Department of Chemical Engineering, Faculty of Engineering, Syiah Kuala University
Jl. Syech Abdurrauf No. 7, Banda Aceh, Indonesia, 23111
E-mail: madi2366@gmail.com

ABSTRAK

Model matematika telah dikembangkan untuk sistem batch dan kontinyu. Pada sistem batch, kinetika adsorpsi oleh monolith berlapis karbon dikaji untuk menganalisis kurva hasil penelitian dengan menggunakan model perkiraan Gaya dorong linear. Kinerja pada kolom monolith dievaluasi melalui kurva output. Model prediksi aliran sumbat yang terdispersi, dengan laju adsorpsinya dinyatakan oleh model tersebut, juga diidentifikasi. Kesetimbangan yang dinyatakan oleh isotermal Langmuir dan parameter laju yang termuat dalam dua persamaan, diperoleh dari penelitian secara batch. Kapasitas adsorpsi monolith karbon aktif tersebut adalah 190 mg/g dan koefisien gaya dorong liniarnya berkurang dari 0,011 menjadi 0,0052 per menit dengan kenaikan konsentrasi awal metilen biru dari 10 hingga 50 ppm. Prediksi yang menggunakan perkiraan gaya dorong linear untuk laju adsorpsi tersebut sesuai dengan data output penelitian.

Kata kunci: adsorpsi, kurva output, gaya dorong linear, kolom monolith, metilen biru

ABSTRACT

Mathematical models of adsorptionon carbon monolithiccolumn for methylene blue removalwere developed for batch and continuous systems. For batch system, kinetics of adsorption by carbon coated monolith was studied to analyze experimental uptake curves by using approximation model oflinear driving force. Performance for monolith column was evaluated through breakthrough curves. A predictive model of dispersed plug flow, with the adsorption rate stated by the model, was also identified. Equilibrium represented by the Langmuir isotherm and rate parameters contained in two equations wasobtained from batch experiment. Capacity of activated-carbon-monolith adsorption was 190 mg/g and linear driving force coefficient decreased from 0.011 to 0.0052 min^{-1} with a rise of initial concentration of methylene blue from 10 toward 50 ppm, respectively. Prediction using linear driving force approximation for adsorption rate fited in with experimental breakthrough data.

Keywords: adsorption; breakthrough curve; linear driving force; monolith column, methylene blue

INTRODUCTION

Activated carbons in the form of powder or granule are commonly implemented in fixed-bed column. Fixed-bed columns have some disadvantages, such as maldistribution (resulting in non-uniform path of adsorbate to adsorbent surface, and non-optimally local conditions), large pressure drop in the bed, and sensitivity toward fouling by impurities. Activated carbon particle should be small in general relating to adsorptive activity. However, smaller particle will result in greater pressure drop (Cybulski and Moulijn, 2006). These disadvantages can be overcome by monolithic structure, which can be considered as a bundle of capillaries having a honeycomb-like shape.

Activated carbon monoliths have been proposed as adsorbent of pollutants from gas stream (Yates *et al*., 2000; Yates *et al*., 2003; Gadkaree, 1998). As compared to gas adsorption, liquid adsorption using activated carbon monolith has received so little attention. Adsorption of methylene blue (MB) using activated-carbon-coated monolith to determine its capacity from aqueous solution has been performed (Darmadi *et al*., 2008).

In this study, the performance for liquid adsorption on the activated carbon coated monolith was investigated by using MB as a model dye. A mathematical model describing adsorption rate on the monolithic column was developed to predict breakthrough curves. Linear driving force (LDF) approximation were used in a batch system. Therefore, no adjustable parameters were required in the model.

MATERIALS AND METHODS

Materials

The materials used in this research were ceramic monoliths (25 mm diameter and 100 mm

length) that were supplied by Beihai Huihuang Chemical Packing Co. Ltd., GuangXi, China. The chemical compositions of the monolithic substrate, as reported by Beihai Huihuang Chemical Packing Co. Ltd., are MgO 13.9 ± 0.5%, SiO_2 50.9 ± 1%, Al_2O_3 35.2 ± 1%, and others < 1%. Monolithic channels' cell shape was square with width of 1.02 ± 0.02 mm, wall thickness of 0.25 ± 0.02 mm, and channel density of 400 cpsi. Monolithic structure of 400 cell per square inch was coated by carbon. Chemicals used in the carbon-coated monoliths were furfuryl alcohol 99% (FA) (Acros Organics, Geel, Belgium), pyrrole 99% (Acros Organics, Geel, Belgium), nitric acid 65% (Acros Organics, Geel, Belgium), and poly ethylene glycol (PEG) with 1500 g/mol molecular weight, further called PEG-1500 (Acros Organics, Geel, Belgium). For adsorption application, standard dye (methylene blue) was used. Powder of the methylene blue was supplied by BDH Gurr-Cersistain, England, then directly utilized without further treatment.

Surface and Pore Volume Analysis

The pore structure (pore volume distribution and Brunauer-Emmett-Teller (BET) surface area) of carbon monolith was measured by nitrogen adsorption at 77 K. The pore volume was calculated by the Barret-Joyner-Halenda (BJH) method.

The specific surface area of porous carbons was usually measured by gas adsorption measurements using the BET theory (Gregg and Singh, 1982). Nitrogen adsorption at 77 K was widely used, although argon at 77 K was also used. For carbon with surface areas less than 5 m^2g^{-1}, krypton at 77 K might be preferably as adsorptive gas because of its low-saturation-vapor pressure (McEnaney and Mays, 1989). Lozano-Castello *et al.* (2004) stated that molecule of nitrogen at 77 K cannot reach the narrowest microporous carbon because of diffusional limitations. Adsorption by using carbon dioxide at 273 K was recommended to obtain complete characterization of the narrowest micropores.

BET developed the first theory to successfully describe multilayer adsorption of gases on a wide range of porous and non porous solids (Do, 1998). For the reason, BET equation was accepted as standard equation in adsorption analysis to obtain specific surface areas of solids. It stated that the first adsorptive layer was localized on surface sites with uniform energy, and subsequent layers were analogous to adsorbate condensation (Gregg and Singh, 1982). Linear form of the BET equation is:

$$\frac{p}{n(p^o - p)} = \frac{1}{n_m c} + \frac{(c-1)}{n_m c} \frac{p}{p^o} \quad \dots \dots \dots \dots \dots \dots \quad (1)$$

where *n* is mole adsorbed at pressure *p* to saturated vapor pressure p^o, n_m is the mole of adsorbate required to cover surface monolayer, and *c* is dimensionless constant given by

$$c = exp\left(\frac{q_1 - q_2}{R_g T}\right) \dots \dots \dots \dots \dots \dots \dots \dots \dots \dots . (2)$$

where q_1 - q_2 is heat of adsorption, q_1 is heat of adsorption in the first adsorbed layer, q_2 is heat of adsorption in subsequent layers, R_g is ideal gas constant, and *T* is temperature.

Polymerization

Polymerization reaction performed in reactor referred to method proposed by Vergunst *et al.* (2002). Monoliths were immersed in polymer solution for 15 minutes. The duration was made shorter compared to previous research which is 24 hours (Mohamad *et al.*, 2014) in order to save immersing time. Optimization by Box-Behnken design was performed to investigate interaction and effects of concentration and molecular weight of PEG, as well as carbonization temperature on pore volume of carbon coated monolith (Darmadi *et al.*, 2009). Characterization of carbon by using thermal-gravimetric analysis, elemental analysis, textural analysis, and scanning electron microscopy had been carried out by Darmadi *et al.* (2009). Amount of carbon coated on monolith after carbonization was about 15.42 wt% of bare monolith.

Kinetic Measurement

Kinetic experiment was conducted in a finite adsorber unit. It is an agitated batch adsorber with a 1.00 L cylindrical glass vessel containing 500 mL liquid. Mixing was provided by a monolithic impeller. The agitator was driven by an Overhead Stirrer Kika Labortechnik Type Rw 20. Study of batch contact time resulted in data of kinetic in curve type of time versus reduced concentration. Carbon-coated monolith of 1.6 g in each experiment was brought into contact with adsorbate solution of 500 mL at different initial adsorbate concentrations of 10, 20, and 50 mg L^{-1}. In regular time intervals, samples of approximately 2 ml were obtained by sampling system, then placed in sample bottles. Withdrawal of the sample was started at t = 0 to 600 minutes every 10 minutes for the first half hour, every 30 minutes for the next an hour and a half, every 1 hour for the rest, then run was terminated. Each of the samples was tested to determine solute concentrations by utilizing UV-vis spectrophotometer at wavelength of 664 nm.

Column Adsorption Studies

Column studies were performed to investigate continuous flow of adsorbate through monolithic column. Adsorption unit was an acrylite column with length of 40 cm and inner diameter of

26 mm. Column was made in particular structure in order to withdraw its samples in different heights (25, 30, and 35 cm) to evaluate breakthrough curve at various bed heights. During research, the column was continuously fed by a 20 mg/L methylene blue solution using peristaltic pump (Ismatec, Ecoline VC-280, Germany). The flow rates were adjusted by setting peristaltic pump switch on rates of 1, 2, and 3, respectively. Up-flow condition was selected to facilitate the accuracy in controlling flow rate of the adsorbate.

Column had been run in three types of flow rate in the range of 1.725 - 4.645 mL/min. The effect of adsorbate concentrations was also investigated by employing 10, 20, and 50 mg/L feed adsorbate concentrations. Samples (~5 mL) were withdrawn in certain interval of time starting from t = 0 to 600 minutes (10 hours). Each sample was tested to determine solute concentrations by utilizing UV-vis spectrophotometer at a wavelength with the maximum absorbance of 664 nm.

Modeling of Adsorption Process

Complete explanation of the mass transfer in adsorbents required solution of partial differential equations (PDEs). The explanation was written by changing equation of diffusion for adsorbent into space-independent approximation in determining rate of adsorption, which was LDF approximation. First, LDF model (Chuang *et al.*, 2005) for batch system was derived with some assumptions: adsorbate concentration throughout bulk of solution in tank is homogeneous; at initial time ($t = 0$), solute concentration is uniform throughout the solution; the adsorbate concentration in its adsorbent at initial time is zero; volume of reactor is constant; the adsorption rate of adsorbate by adsorbent is linearly proportional to driving force, stated as a difference between concentration of surface and average concentration of adsorbed-phase; and system is isothermal. Mass conservation equation in batch condition is stated as:

$$-V \frac{dC}{dt} = M \frac{d\overline{q}}{dt} \qquad \text{……………...….. (3)}$$

C is the concentration in liquid phase (mg/L), V is liquid volume (L), M is the mass of adsorbent (g), and $\overline{q}$ is average concentration of adsorbed phase per unit mass of adsorbent (mg/g). In solid phase, the average concentration is given by LDF approximation (Gleuckauf, 1955):

$$\frac{d\overline{q}}{dt} = k_{LDF} (q^* - \overline{q}) \qquad \text{……………...….. (4)}$$

where q^* is concentration of the adsorbed phase at particle surface in equilibrium with bulk

concentration (mg/g), and k_{LDF}, LDF kinetic constant (1/s), is given by (Zabka *et al.*, 2006):

$$k_{LDF} = \frac{8D_{eff}R_1^2}{(R_1^2 - R_2^2)^2} \qquad \text{……………….. (5)}$$

where D_{eff} is pore diffusion (m²/s), R_1 is monolith radius (m), R_2 is radius of the monolith channel wall (m).

For square channel, Patton *et al.* (2004) gives:

$$R_1 = \frac{2a}{\pi} \qquad \text{…………………………...….. (6)}$$

and

$$R_2 = \sqrt{\frac{4t_w}{\pi}(t_w + a) + R_1^2} \qquad \text{……………...……. (7)}$$

where a is diameter of the monolithic channel (m) and t_w is the thickness of carbon coated (m).

Performance of a monolithic column is analyzed by studying its breakthrough which is outlet responses of a monolith bed toward inputs. In order to derive mathematical model of carbon monolithic column, the following assumptions are used: uniform flow distribution in the monolithic column; unvaried parameters of mass transfer and physico-chemical properties throughout monolithic column; each channel is identical; carbon is initially free of adsorbate; isothermal operation; radial diffusion is ignored; and mass transfer within the adsorbent is described by LDF model. Using above assumptions, material balance in bulk phase of a monolithic channel gives:

$$\frac{\partial C}{\partial t} = -v_z \frac{\partial C}{\partial z} + D_{ax} \frac{\partial^2 C}{\partial z^2} - \frac{(1-\varepsilon_m)}{\varepsilon_m} \frac{\partial \overline{q}}{\partial t} \qquad \text{………... (8)}$$

where C is concentration of bulk liquid phase (kg/m³), z is axial coordinate (m), t is time (s), v_z is interstitial velocity of fluid in monolithic channel (m/s), ε_m is monolithic structure porosity, and D_{ax} is axial dispersion coefficient (m²/s).

The boundary and initial conditions are

$$C(t = 0, z) = 0, \quad and \quad \overline{q}(t = 0, z) = 0 \quad \text{........ (9)}$$

$$C(t, z = 0) = C_F \qquad \text{.. (10)}$$

$$\frac{dC}{dz}(t, z = L) = 0 \quad \text{... (11)}$$

where C_F is initial concentration (kg/m^3). Dispersion coefficient, D_{ax}, can be represented by (Douglas, 1984):

$$D_{ax} = \gamma_1 D_{eff} + \gamma_2 \, a \, v_z \quad \text{............................... (12)}$$

where γ_1 and γ_2 are geometrical constants. For monolithic channel, (Zabka *et al*., 2006) gives $\gamma_1 = 0.85$ and $\gamma_2 = 3.68$, respectively. The governing Equation (8) and Equation (12) are developed by combining effects of adsorption equilibrium, mass transfer, and dispersion. Information concerning adsorption equilibrium for adsorbate-adsorbent system is provided by measurements made in batch studies. The LDF mass transfer coefficients (k_{LDF}) are obtained from matching a batch model with experimental uptake rate data. Column model is then used to predict breakthrough curves in a monolithic column. Note that the model does not have any adjustable parameter.

Numerical Simulation

The column model described previously is non-linear PDE. The PDE was discretized in spatial domain with orthogonal collocation (OC) method (Villadsen and Michelsen, 1978; Richard and Duong, 2012; and Choong *et al*., 2006). This set of ordinary differential equations (ODEs) was solved by using MATLAB subroutine ODE15s. It was found that twenty (20) interior collocation points give balance between computational speed and accuracy. In assuring appropriateness of the OC method, discrete scheme was verified by heat conduction in finite slab and plug flow-adsorption-model cases, and analytical solutions. Conformity for both cases was excellent.

In order to solve Equation (3), equilibrium adsorption capacity and initial conditions have to be known. The governing Equation (3) and Equation (4) from a set of ODEs, are solved simultaneously to obtain concentration of fluid phase as a function of time. The linear driving force mass transfer coefficient (k_{LDF}) is determined by matching simulation with experimental data.

RESULTS AND DISCUSSION

Specific surface area and pore volume for the carbon monolith are indicated in Table 1. These results confirm that the carbon monolith has relatively low specific surface. The equilibrium relationship between the activated carbon monolith and dye are described well by using the Langmuir isotherm:

$$q^* = \frac{19.13 C^*}{1 + 0.1 C^*} \quad \text{……………….…..…..….. (13)}$$

where C^* is concentration in the bulk fluid phase (mg/L).

The linear driving force mass transfer coefficients (k_{LDF}) are extracted by solving Eq. 3 for batch system in both average concentration in solid phase and initial concentration. Then solution obtained is matched with kinetic data (Fig. 1). The best fit values are then listed (Table 2). Based on correlation coefficients, R^2 for monolith, the monolith can be considered as better adsorbent that carbon coated monoliths 8000 whose R^2 is 0.978 (Yi *et al*., 2013).

It is evident that k_{LDF} and D_{eff} depends on initial concentration. Both k_{LDF} and D_{eff} decrease with an increase of dye concentration. It indicates that there is an increase of affinity energy with progressive filling of site. Therefore, dye is strongly bonded to adsorbent surface, which reduces its diffusion rate from site to site (Abd *et al*., 2010). Adsorption capacity obtained is 190 mg/g (relatively larger than capacity of methylene orange, i. e. 28 − 132.7 mg/g (Willie *et al.*, 2013), and much higher compared to that of β-carotene, i. e. 62.118 mg/g (Muhammad *et al*., 2011).

Table 1. Specific surface area and pore volume for carbon monolith tested in nitrogen adsorption at temperature of 77 K

Sample	S_{BET} (m^2/g$_{carbon}$)	Total pore volume (cm^3/g$_{carbon}$)	Mesopore area (m^2/g$_{carbon}$)	Mesopore volume (cm^3/g$_{carbon}$)
Activated Carbon	431.0000	0.3800	186.5500	0.2313

Table 2. Parameters of LDF model for adsorption of MB at various initial concentrations

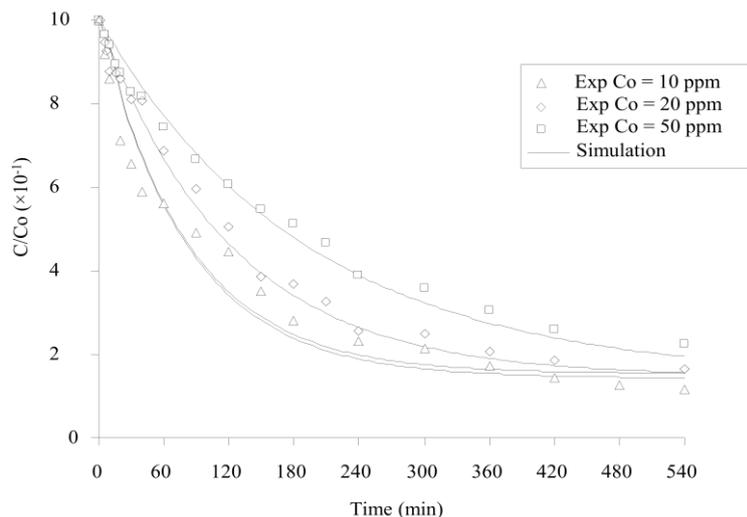| Initial Conc. (ppm)	k_{LDF} (min^{-1})	$D_{eff} \times 10^8$ (cm^2 s^{-1})	R^2
10	0.01100	6.932	0.9865
20	0.00825	6.661	0.9974
50	0.00520	4.199	0.9945

Figure 1. Plot of the MB removal versus time for different initial concentrations: Δ k_{LDF} = 0.0110 min^{-1}; $\Diamond$ k_{LDF} = 0.00825 min^{-1}; $\Box$ k_{LDF} = 0.00520 min^{-1}.

Breakthrough curve in each experiment is resulted from the experiment concentration versus time data. Figure 2 depicts breakthrough curves for MB removal with carbon coated monolith at three different dye feed concentrations, 30 cm height of bed, and 1.725 mL/min rate of flow. Shape difference observed at the breakthrough curve is ascribed to varied adsorption-driving-force because this system has the same flow rate, i.e. the same hydraulic loading. Breakthrough curves are flatter in low concentrations, which indicates mass transfer zone that is relatively wider, and film-controlled process. Conversely, an increase of initial adsorbate concentration increases slope of the breakthrough curve that reduces time needed before generation of carbon. It indicates that concentration change at the beginning could modify rate of adsorption and breakthrough time, hence difussion process depends on concentration (Foo and Hameed, 2012).

At constant flow rate, an increase of dye concentration reduces throughput until breakthrough. This is because high adsorbate concentration makes carbon saturated more quickly, so that decreases breakthrough time. It can be concluded that higher dye concentrations reduce the treating times because carbon coated monolith is saturated more quickly (Walker and Weatherley, 1997). The results indicates that the modeling is favorable because there is relationship between concentration at the beginning with brakthrough time, not as for phenol adsorption (Anisuzzaman *et al.*, 2014).

Breakthrough curve at different bed heights are indicated as plot of the dimensionless concentration versus time (Figure 3). It indicates that adsorber capacity increases at higher bed-depths or carbon mass. It also confirms that volume of solution treated and adsorbate removal increases as bed depth increases (Hasfalina *et al.*, 2012). This behavior is favorable since higher carbon mass means that there are more available adsorption sites for MB. However, breakthrough curves indicated in Figure 3 do not look like typical profile of "S-shape" that is resulted in ideal adsorption system. Similar patterns of breakthrough curves are obtained for adsorption of reactive dyes, tectilon red 2B, tectilon blue 4R-01, as well as tectilon orange 3G with adsorber of Filtrasorb 400, and for adsorption of acid dye using granular activated carbon (Walker and Weatherley, 2000; Al-Degs *et al.*, 2007).

Deformed breakthrough curves are attained because of two reasons: (1) adsorption kinetics of MB are slow on carbon coated monolith that is porous, where slow MB kinetics makes breakthrough faster, consequently results in "S" breakthrough shape that is incomplete, and (2) utilization of small scale-column-apparatus commonly results in adsorption breakthrough curve (Al-Degs *et al.*, 2007; Crittenden *et al.*, 2005). Zone of adsorption along bed decreases throughout the bed height at particular rate which suggests that higher bed height is probably necessary for dye adsorption.

The tendency takes place at adsorption of dye material as a result of its large molecular structure so that its resistance toward internal diffusion is extremely higher compared to that of smaller molecular structures such as phenol. Breakthrough curves for three types of flow rate, 30 cm fixed bed height, and 20 ppm initial concentration are indicated in Figure 4. Breakthrough curve shape indicates internal resistance in column, as well as relative effect in mass transfer parameter for all conditions of operation. Apparently, breakthrough point occurs earlier at higher flow rates, implying shorter column life.
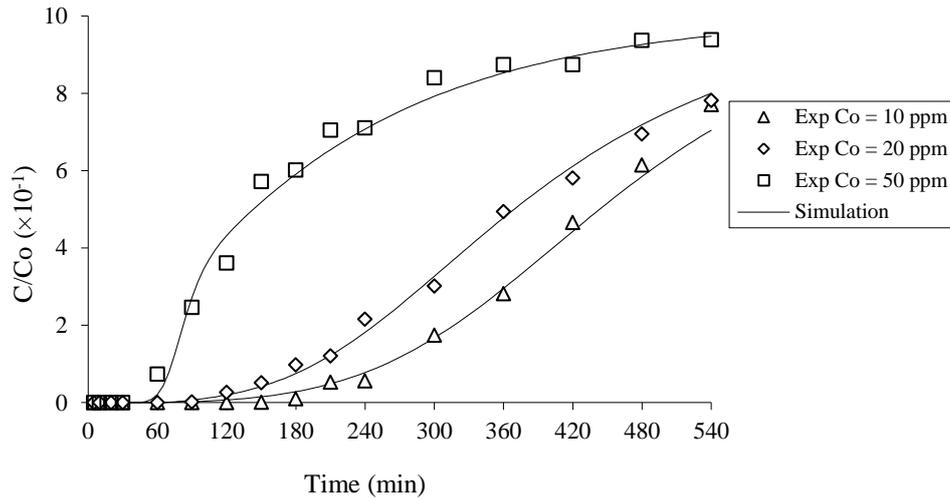
Figure 2. Breakthrough curve for different feed dye concentrations, 30 cm height of bed, and 1.725 mL/min rate of flow
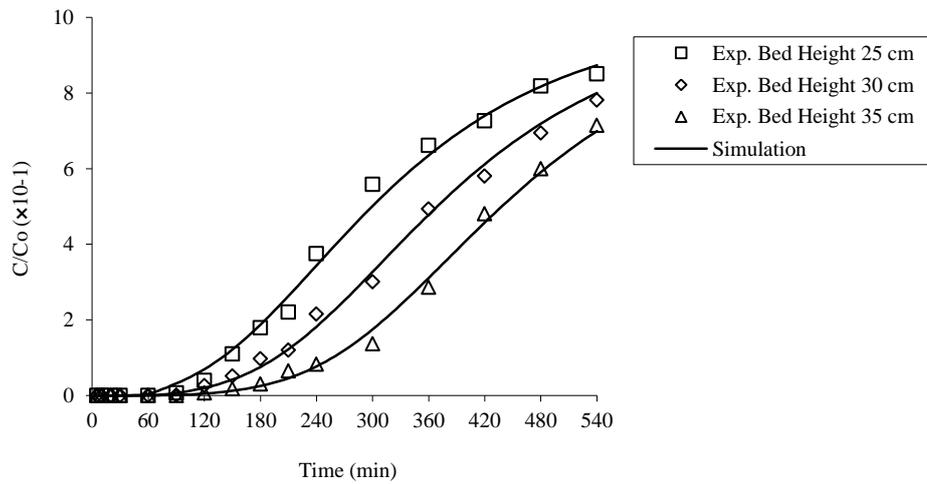

Figure 3. Breakthrough curves of MB adsorption on various bed heights at 1.725 mL min^{-1} flow rate, 2.5 pH, and C_0 of 20 ppm
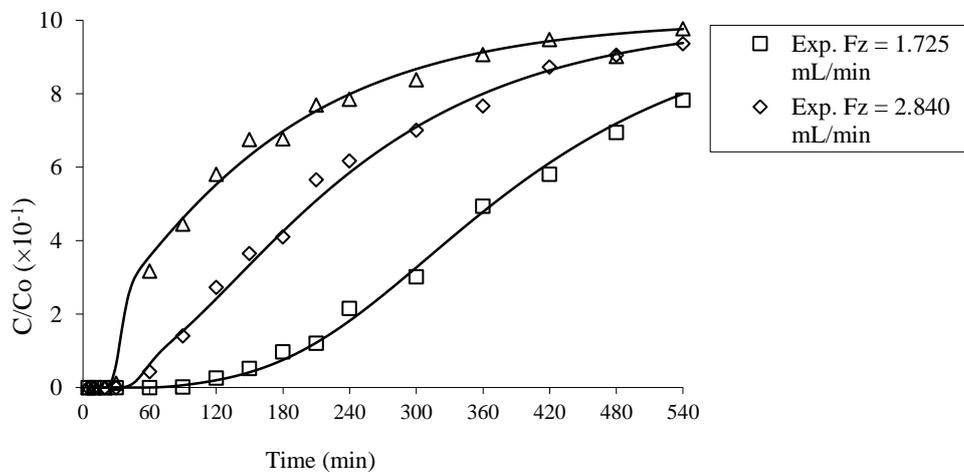

Figure 4. Breakthrough curves of MB adsorption on various flow rates, 20 ppm feed concentration, bed height of 30 cm, and pH of 2.5.

Breakthrough curves are also premature in larger flow rates, indicating that rate of adsorption is controlled by internal diffusion, and a narrow mass transfer zone occurs (Ahmad *et al*., 2007). It is also because of decrease in contact time between adsorbent and dye at higher flow rate (Walker and Wetherley, 1997). Besides, it is attributable to insufficient contact time of adsorbate in column to enable adsorbate diffuse into monolith pores (Salman *et al*., 2011). Therefore, solution weakly spreads or diffuses into monolith particle that causes time quicker to achieve saturation, or lower efficiency (Mohammad *et al*., 2012).

Breakthrough curves are flatter for lower rates indicating that effect of film resistance is more prominent, service time of the bed is longer, and zone of mass transfer is larger. It is reasonable because boundary layer around particles is thicker in lower flow rate that it increases external mass transfer resistance. It also indicates that adsorption is incomplete and leads to steep breakthrough result in initial operation (Ai and Ahmad, 2014). Effects of process parameters on breakthrough curve are also investigated. Breakthrough curves for all parameters are not like characteristic of 'S' shape profile resulted in ideal adsorption system; it is connected to adsorbate molecular size. Most research performed on adsorption of dyes indicates similar profile of breakthrough curves to profile reported here. It appears that simulations performed by predictive model fits very well to the experimental breakthrough curve (Figures 2 - 4).

CONCLUSIONS AND RECOMMENDATION

Conclusions

LDF model for monolithic system was developed to extract LDF mass transfer coefficients (k_{LDF}) by fitting the simulation to experimental data of uptake rate. Comparison of results by the LDF model and experiment was good with k_{LDF} of 1.10×10^{-2}, 8.25×10^{-3}, and 5.20×10^{-3} min^{-1} at concentrations of 10, 20, and 50 mgL^{-1}, respectively. A predictive model of dispersed plug flow, with adsorption rate stated by the LDF model, was developed to estimate breakthrough curve of monolith column. Parameters of the model were determined by batch adsorption experiments. Simulation result obtained fits well to the experiment. Optimization could carried out with respect to geometric properties of the monolithic cell density and thickness of carbon coating layer. The LDF model employed in this work had its limitations as it assumes space independent approximation for the rate of adsorption. It is interesting to consider some of new rate models for adsorption. Activated carbon monolith was usable in other processes, i.e. recovery of beta-carotene from palm oil, multi-component dye adsorption, and catalyst support in

hydrogenation reaction. Investigation of desorption and regeneration of activated carbon monolith is required.

Recommendation

Optimization can be carried out with respect to geometric properties of the monolithic cell density and thickness of carbon coating layer. The LDF model applied in this research should be replaced with new models e.g. film-pore-concentration-dependent-surface-diffusion model. Activated carbon monolith is usable in recovery of beta-carotene from palm oil, multi-component dye adsorption, and catalyst support in extremely exothermic reaction. Furthermore, investigation of desorption and regeneration of activated carbon monolith is also required in the future.

REFERENCES

Abd MME, Amal MI, and El-Kady MF. 2010. Adsorption Equilibrium, kinetics and thermodynamcs of methylene blue from aqueous solutions using biopolymer oak sawdust composite. *J Am Sci*. 6: 267-283.

Ahmad J, Lam SS, Nora'aini A, Noor MJMM. 2007. A simulation study of the removal efficiency of granular activated carbon on cadmium and lead. *Desalination*. 206: 9-16. doi:10.1016/j.desal.2006.04.048

Ai PL and Ahmad ZA. 2014. Continuous fixed-bed column study and adsorption modeling: Removal of cadmium (II) and lead (II) ions in aqueous solution by dead calcareous skeletons. *Biochem Eng J*. 87: 57-61, doi 10.1016/j.bej.2014.03.019.

Al-Degs Y, Khraisheh MAM, Allen SJ, Ahmad MN, Walker GM. 2007. Competitive adsorption of reactive dyes from solution: Equilibrium isotherm studies in single and multisolute systems. *Chem Eng J*. 128: 163-167.

Anisuzzaman SM, Awang B, Duduku K, Yit ZT. 2014. A study of dynamic simulation of phenol adsorption in activated carbon packed bed column. *J King Saud Univ – Eng Sci*. Article in press, doi 10.1016/j.jksues.2014.01.001.

Choong TSY, Wong TN, Chuah TG, Idris A. 2006. Film pore concentration dependent surface diffusion model for the adsorption of dye onto palm kernel shell activated carbon. *J of Colloid and Interface Sci*. 301: 436-440.

Chuang CL, Fan M, Xu M, Brown RC, Sung S, Saha B, Huang CP. 2005. Adsorption of arsenic(V) by activated carbon prepared from oat hulls. *Chemosphere*. 61: 478-873. doi:10.1016/j.chemosphere.2005.03.012

Crittenden B, Patton A, Jouin C, Perera S, Tennison S, Echevarria JAB. 2005. Carbon

monoliths: A comparison with granular materials. *Adsorption*. 11: 537-541.

Cybulski A and Moulijn JA. 2006. *Structured catalysts and reactors*. 2nd Ed. Boca Raton. Florida: Taylor & Francis Group.

Darmadi, Choong TSY, Chuah TG., Yunus R, Taufik Yap YH. 2008. Adsorption of methylene blue from aqueous solutions on carbon coated monolith. *Asean J Chem Eng*. 8: 27-38.

Darmadi, Choong TSY, Chuah TG, Yunus R, Taufiq Yap YH. 2009. Development of polymer derived carbon coated monolith for liquid adsorption application by response surface methodology. *The Canadian J Chem Eng*. 87: 591-597.

Do DD. 1998. *Adsorption Analysis: Equilibria and Kinetics*. Imperial College Press: London.

Douglas MR. 1984. *Principles of Adsorption and Adsorption Processes*. New York: John Wiley & Sons Inc.

Foo KY and Hameed BH. 2012. Dynamic adsorption behavior of methylene blue onto oil palm shell granular activated carbon prepared by microwave heating. *Chem Eng J*. 203: 81-87.

Giovanna F, Erc SF, and Stafano B. 2009. Multicriteria design framework for CO_2 capture by multi-step PSA Cycles. *19th European Symposium on Computer Aided Process Engineering*. Amsterdam: Elsevier.

Gregg SJ and Singh KSW. 1982. *Adsorption, Surface Area and Porosity*. Academic Press. London.

Hasfalina CM, Maryam RZ, Luqman CA, Rashid M. 2012. Adsorption of Copper (II) from Aqueous Medium in Fixed-Bed Column by Kenaf Fibres. *APCBEE Procedia*. 3: 255-263. doi 10.1016/j.apcbee.2012.06.079.

Lingai L, David R, Mark JR, Georges G. 2006. Adsorption and electrothermal desorption of organic vapors using activated carbon adsorbents with novel morphologies, *Carbon*. 44: 2715-2723. doi:10.1016/j.carbon.2006.04.007.

Lozano-Castello D, Cazorla AD, Linares-Solano A. 2004. Textural development and hydrogen adsorption of carbon materials from PET waste. *J Alloys Compd*. 379: 280-289.

McEnaney B and Mays TJ. 1989. *Introduction to Carbon Science*, edited by Marsh H. Butterworths.

Mohamad RM, Moonis AK, Soraya H, Luqman CA, Thomas SYC. 2014. Adsorption/desorption of cationic dye on surfactant modified mesoporous carbon coated monolith: Equilibrium, kinetic and thermodynamic studies. *J Industand Eng Chem*. Article in press, doi 10.1016/j.jtice.2012.07.001.

Mohammad AS, Zahra H, Mohd HSI, Norhafizah A. 2012. Continuous metal and residual oil removal from palm oil mill effluent using natural zeolite-packed column. *J Taiwan Institute of Chem Eng*. 43: 934-941, doi 10.1016/j.apcbee.2012.06.079.

Muhammad, Moonis AK, Thomas SYC, Chuah TG, Robiah Y. 2011. Desorption of β-carotene from mesoporous carbon coated monolith: Isotherm, kinetics and regeneration studies. *Chem Eng J*. 173: 474-479, doi10.1016/j.cej.2011.08.015.

Muhammad, Thomas SYC, Chuah TG, Robiah Y, Taufiq YHY. 2010. Adsorption of β-carotene onto mesoporous carbon coated monolith in isopropyl alcohol and *n*-hexane solution: equilibrium and thermodynamic study. *Chem Eng J*. 164: 178-182, doi 10.1016/j.cej.2010.08.052.

Patton A, Crittenden BD, Perera SP. 2004. Use of the linear driving force approxi-mation to guide the design of monolithic adsorbents. *Chem Eng Res and Design*. 82: 999-1009.

Richard GR and Duong DD. 2012. *Applied Mathematics and Modeling for Chemical Engineers*. New York: John Wiley & Sons. Inc.

Salman JM, Njoku VO, and Hameed BH. 2011. Batch and fixed-bed adsorption of 2,4-dichloroohenoxyacetic acid onto oil palm frond activated carbon, *Chem Eng J*. 174: 33-40, doi 10.1016/j.cej.2011.08.024.

Soraya H, Thomas SYC, and Muhammad H. 2012. Adsorption of a cationic dye from aqueous solution on mesoporous carbon-based honeycomb monolith. *Desalination and Water Treatment*. 49: 326-336, doi: 10.1080/19443994.2012.-719359.

Vergunst T, Kapteijin F, and Moulijin JA. 2002. Preparation of carbon-coated monolithic supports. *Carbon*. 40: 1891-1902.

Villadsen J and Michelsen ML. 1978. *Solution of Differential Equation Model by Polynomial Approximation*. Englewood Cliffs. New Jersey: Prentice-Hall. Inc.

Walker GM and Weatherley LR. 1997. Adsorption of acid dyes onto granular activated carbon in fixed beds. *Water Res*. 31: 2093 – 2101.

Willie C, Soraya H, Moonis AK, Chuah TG, Thomas SYC. 2013. Acid modified carbon monolith for methyl orange adsorption. *Chem Eng J*. 215-216: 747-754, doi 10.1016/j.cej.2012.07.004.

Xin Z, Ying W, Cuimiao F, Ying S, Dongyuan Z. 2009. Highly efficient adsorption of bulky dye molecules in wastewater on ordered mesoporous carbons. *Chem Matter*. 21: 706-716, 10.1021/cm8028577.

Yates M, Blanco J, Avila P, Martin MP. 2000. Honeycomb monoliths of activated carbons

for effluent gas purification. *Microp and Mesop Mat.* 37: 201-208.

Yates M, Blanco J, Martin-Luengo MA, Martin MP. 2003. Vapour adsorption capacity of controlled porosity honeycomb monoliths. *Microp and Mesop Mat.* 65: 219-231.

Yi PT, Moonis AK, and Thomas SYC. 2013. Kinetic and isotherm studies for lead adsorption from aqueous phase on carbon coated monolith. *Chem Eng J.* 217: 248-255, doi 10.1016/j.cej.2012.12.013.

Zabka M, Minceva M, and Rodrigues AE. 2006. Experimental and modeling study of adsorption in preparative monolithic silica column. *Chem Eng and Proces.* 45: 150 – 160.